

Chapter 1

Introduction

1.1.- Antiferromagnetic and Ferromagnetic Materials: Soft and Hard

Some magnetic phenomena, like the ability of certain materials to attract pieces of iron or the property of being oriented under the action of a magnetic field have been known and used for hundreds of years. However, the extensive application of magnetic materials did not come until the last century. Some well-known examples where magnetic materials are commonly used are electronic devices, suspension mechanisms, radio or TV equipments or motors, among many others [1].

All materials that exist in nature can be classified into different categories, depending on their response to an applied magnetic field, H . Some of the types of magnetic behaviour are ferromagnetism, ferrimagnetism, antiferromagnetism, paramagnetism or diamagnetism. From a classical microscopic point of view, this is due to the existence of magnetic moments associated either with the movement of electrons around the atomic nucleus (orbital angular momentum, which gives rise to the angular moment) or rotation of electrons around their own axis (spin angular momentum, which gives rise to the spin moment).

In *ferromagnetic* (FM) materials, the magnetic moments tend to align parallel to each other within certain regions (domains). This effect originates a spontaneous magnetization. If a large enough magnetic field is applied, the magnetization of the different domains align with each other and the net magnetization reaches a constant value, i.e. the so-called *saturation magnetization*, M_S . Moreover, another characteristic of FM materials is that when the magnetic field is removed, some magnetic moments remain aligned in the direction of the previous magnetizing field, originating a *remanent magnetization*, M_R . The negative magnetic field required to reduce M back to zero is denoted as *coercivity*, H_C . A completely analogous behaviour is encountered when the material is saturated in negative magnetic fields. The whole curve obtained when plotting M vs. H is called *hysteresis loop* [1-5].

On the other hand, in the materials designated as *antiferromagnetic* (AFM), the magnetic moments tend to align antiparallel to each other. In this case, the net spontaneous magnetization is essentially zero and they do not exhibit any hysteretic behaviour, i.e. when plotting M vs. H a linear graph is obtained. In *paramagnetic* (PM) materials, the magnetic

moments do not interact with each other so that, in absence of a magnetic field, they are oriented at random. However, when a field is applied, to a certain extent, the moments tend to align to it. The typical magnetization curves of FM, AFM and PM materials are shown in figure 1.1.

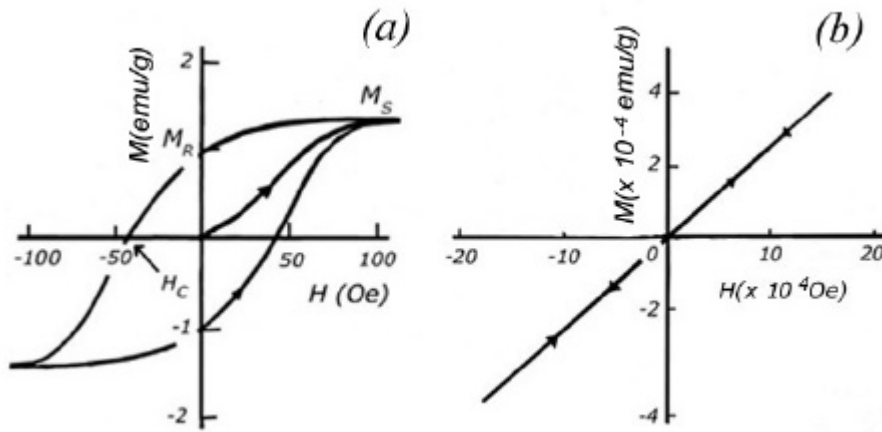


Figure 1.1: Typical magnetization curves for (a) a FM material and (b) a PM or AFM material.

It is noteworthy that when FM or AFM materials are heated, the thermal energy causes their magnetic moments to oscillate in such a way that they tend to lose their magnetic ordering, becoming both of them PM. The temperature at which this transformation occurs is called Curie temperature, T_C (in FM materials) or Néel temperature, T_N (in AFM materials).

The large variety of ferromagnetic materials that exist in nature can be roughly classified into two categories: soft and hard ferromagnetic materials. Soft ferromagnetic materials are characterized by low values of H_C , typically lower than 10 Oe, and large values of M_S , usually higher than 100 emu/g. This results in a narrow hysteresis loop (see fig. 1.2 (a)). Some examples of soft FM materials are Fe, Ni, permalloy or FeSi alloys. They are used in, for example, electromagnets or transformers cores. On the contrary, hard FM materials, which are also known as *permanent magnets*, are characterized by high values of H_C , typically larger than 350 Oe, and usually smaller values of M_S than soft magnetic materials, i.e. wide hysteresis loops (see fig. 1.2 (b)). Some examples of hard FM are SmCo₅, Al-Ni-Co alloys or Nd₂Fe₁₄B. Permanent magnets have lots of applications in industry: for example in the fabrication of motors and generators, in telecommunications (headphones, magnetic sensors, high-density magnetic recording media, ...), in synchrotrons (as systems for elemental particles guidance), etc. [6].

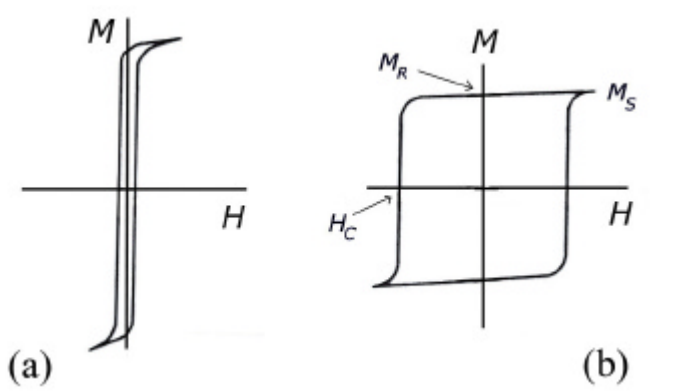


Figure 1.2: Hysteresis loops of (a) a soft magnetic material and (b) a hard magnetic material.

The figure of merit of a hard magnetic material is its *energy product*, which is denoted by $(BH)_{Max}$, and is roughly proportional to the total area enclosed by the hysteresis loop, when plotting the magnetic induction, B , i.e. $B = H + 4\mu M$, as a function of H . $(BH)_{Max}$ gives a good estimation of the quality of the hard magnetic material, since it is closely related to the overall energy that can be stored in the magnet. Obviously, magnets with higher $(BH)_{Max}$ would require smaller sizes to have the same efficiency.

In order to maximize $(BH)_{Max}$ it is necessary to have a large H_C , high values of M_S and a squareness ratio, M_R/M_S , as close to 1 as possible. Shown in fig. 1.3 are the effects of increasing each of these three parameters, while keeping the remaining ones constant, on the area of a hysteresis loop and, hence, on the energy product of the magnet. The result of increasing H_C is a widening of the hysteresis loop (see fig. 1.3 (a)), while increasing M_S results in a lengthening of the loop along the magnetization axis (fig. 1.3 (b)). Finally, an increase of M_R/M_S makes the loop more square (fig. 1.3 (c)). The net effect in all three cases is an enhancement of the energy product.

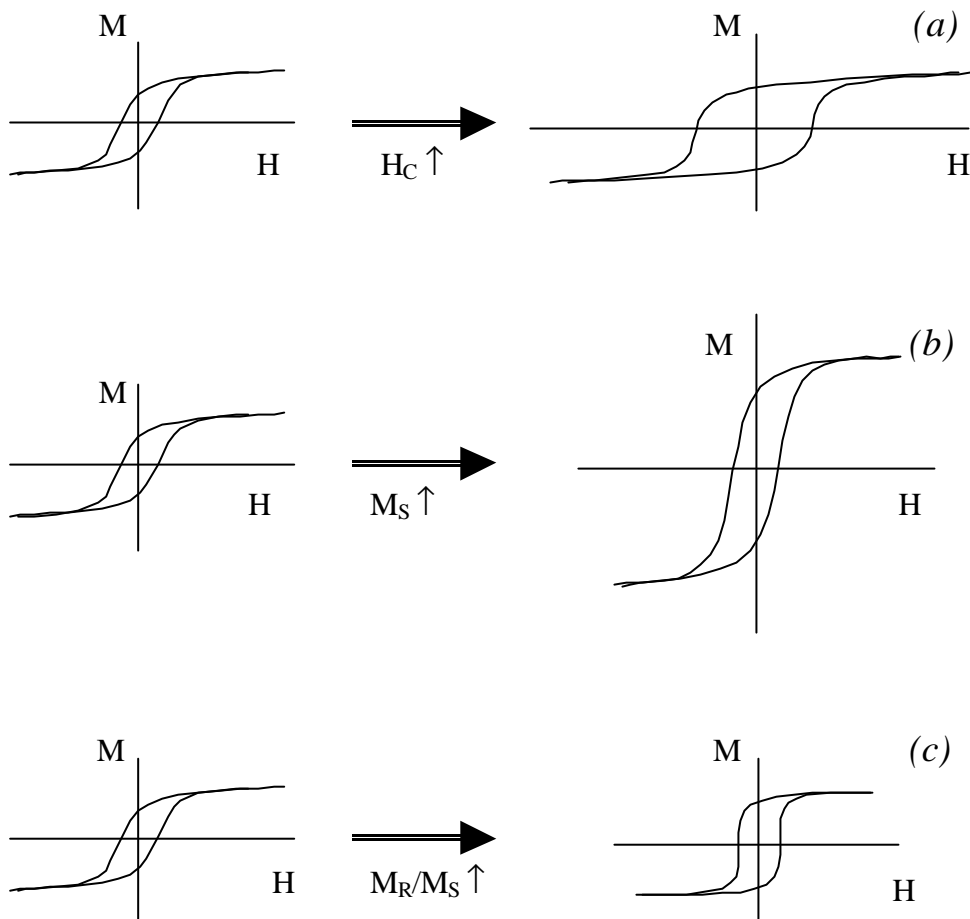


Figure 1.3: Effect of increasing (a) the coercivity, (b) the saturation magnetization or (c) the squareness ratio on the hysteresis loop. Note that in the three cases the net effect is an increase of the total area enclosed by the hysteresis loop.

Figure 1.4 shows the enhancement of $(BH)_{Max}$ that has been accomplished during the last century in different types of hard FM materials.

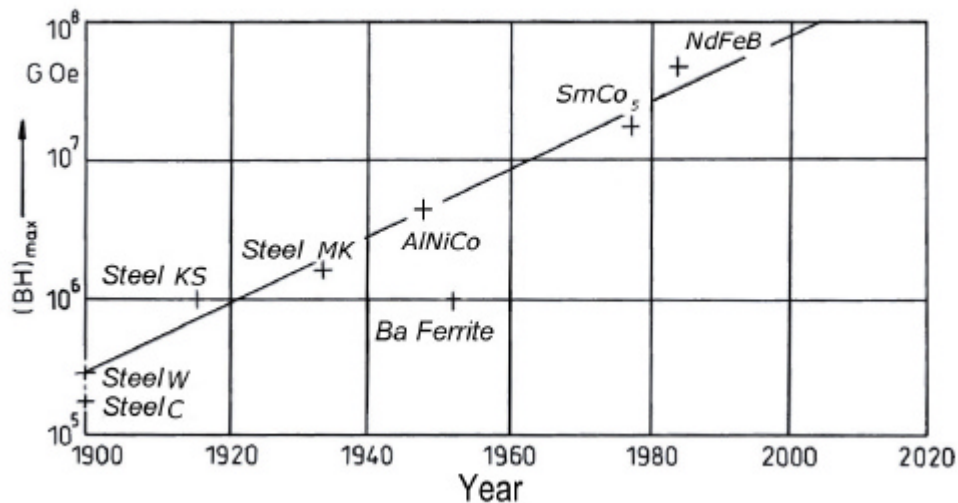


Figure 1.4: Chronological evolution of the energy product values, at room temperature, in permanent magnetic materials during the last century.

1.2.- Conventional Hard Magnetic Materials:

1.2.1.- Ferromagnetic materials consisting of a single ferromagnetic phase

Traditionally, the most commonly used permanent magnetic materials have been hardened steels, Al-Ni-Co alloys and Ba or Sr ferrites. However, during the last 30 years, new materials have emerged, such as SmCo_5 or $\text{Nd}_2\text{Fe}_{14}\text{B}$, in which $(BH)_{Max}$ has been enhanced by one or two orders of magnitude. Except for AlNiCo, all these materials are essentially monophasic. Single-phase magnets, based on rare-earth intermetallics, were first developed more than 20 years ago, usually by crystallization from an amorphous precursor, either by ball milling or by melt spinning and subsequent heat treatments [7-10]. Typical values of H_C of around 15 kOe were obtained in $\text{Nd}_2\text{Fe}_{14}\text{B}$, for grain sizes around 80 nm.

There are several important factors that affect the properties of magnets consisting of a single ferromagnetic phase, such as the crystallite size, magnetic anisotropy, orientation, particle shape or exchange interactions.

- (i) The control of the crystallite size, in the nanometric range, plays a very important role when trying to achieve large values of $(BH)_{Max}$ [6]. As can be seen in figure 1.5, for non-interacting FM particles, a maximum is obtained when the coercivity, H_C , is plotted as a function of the crystallite size, $\langle d \rangle$. For large values of $\langle d \rangle$, when the

direction of H is reversed, the magnetization changes from positive to negative values, due to the formation and motion of domain walls. However, if the crystallite size is reduced to $\langle d \rangle_C$, the formation of domain walls becomes energetically unfavourable, so that the particles are in a single-domain state. Consequently, the magnetization reverses by means of coherent rotation of spins, resulting in a high value of H_C . If $\langle d \rangle$ is further reduced to below $\langle d \rangle_C$, thermal fluctuations cause some magnetic disorder in the FM and H_C is progressively reduced. Finally, if $\langle d \rangle$ is low enough the system becomes superparamagnetic and no hysteresis is observed. This happens when $25k_B T \gg KV$, where k_B is the Boltzmann constant, T is temperature, K is the magnetic anisotropy of the FM and V is the volume of the FM particle. This condition is commonly known as the *superparamagnetic limit*. Superparamagnetic behavior has been studied by many authors [11,12].

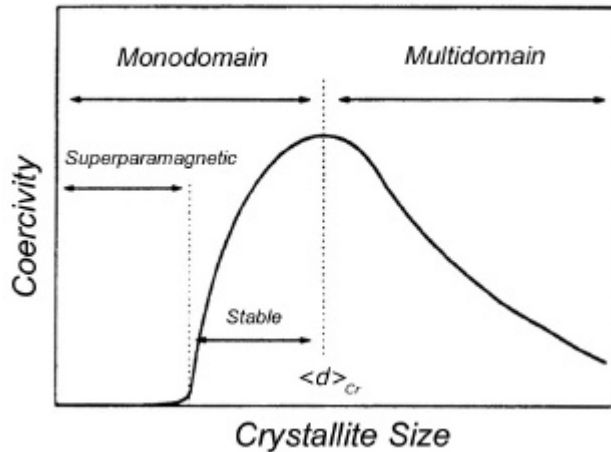


Figure 1.5: Dependence of the coercivity on the crystallite size, $\langle d \rangle$, for a FM material [6].

(ii) The role of the magnetic anisotropy can be estimated in a first approximation by the Stoner-Wohlfarth model [13], which assumes coherent rotation of the spins in monodomain, non-interacting particles, with uniaxial anisotropy. According to this model:

$$H_C = \frac{2K}{M_s} \quad (1.1)$$

where K is the uniaxial anisotropy constant and M_s is the saturation magnetization of the material. Usually, the constant K is related to the structure of the material

(*magnetocrystalline anisotropy*). Magnetocrystalline anisotropy is an intrinsic property of the material. In the demagnetised state, depending on the crystalline structure there are one or more directions towards which the spins tend to align preferably. These directions are denoted as *easy axis*. When a magnetic field is applied, a certain work is required in order to move the spins out of the easy axis direction. Therefore a certain energy, called anisotropy energy, is stored in the magnet when the magnetic field is applied in a direction different from the easy axis. The magnitude of the anisotropy energy depends on a certain number of anisotropy constants (K_0 , K_1 , K_2 , etc.), which vary both with the crystalline structure of the material and the temperature of experiment. However, other types of magnetic anisotropies (e.g. shape anisotropy or anisotropies due to mechanical tensions, plastic deformation or irradiation by electrons, X-rays, ions, etc.) can also have some influence on the value of K . From equation (1.1) it is clear that a possible way to enhance $(BH)_{Max}$ is to look for materials with high values of K , so that their H_C becomes also large.

- (iii) The effect of orientation can be also examined in terms of the Stoner-Wohlfarth model [13]. This model predicts that for isolated non-interacting single-domain particles oriented at random the remanent magnetization takes the value $M_R = M_S / 2$. This result is the consequence of the fact that, when the applied magnetic field is removed, the spins of each particle align along the easy axis direction of the particle, leading to a value of M_R lower than M_S , given by:

$$M_R = M_S \langle \cos(\mathbf{q}) \rangle \quad (1.2)$$

where \mathbf{q} is the angle between the easy axis and the magnetic field. In the particular case of random orientation one obtains, after averaging $\langle \cos(\mathbf{q}) \rangle$, that $M_R = M_S / 2$. Therefore, in order to maximize M_R/M_S , a magnetic field is often used during the processing route to align the particles and thus make the magnet anisotropic, obtaining M_R very close to M_S .

- (iv) As mentioned, apart from the magnetocrystalline anisotropy, which is an intrinsic property of the magnetic material, other types of anisotropies can also play some role in tuning the properties of hard magnets. Among them, shape anisotropy is one of the most important. This anisotropy has its origin in the different magnetostatic energies encountered when the particles are magnetized in different directions. This is due to their shape. For example, in the Alnico-type permanent magnets, annealing and field cooling from above 900 K results in the formation of a microstructure consisting of elongated FM FeCo particles embedded in a non-magnetic NiAl matrix. In AlNiCo an

optimum magnetic behaviour (e.g. highest H_C and M_R) is obtained when the acicular FeCo regions are of about 15 nm in diameter and 150 nm in length. Shape anisotropy is also the source of large coercivities in small particles of nanocrystalline Fe or CrO_2 [2-4].

- (v) Furthermore, in real magnets, adjacent particles usually interact with each other. The exchange interactions between different FM grains bring about a decrease of the coercivity, since cooperative reversal of M of several grains can be encountered. Therefore, a good method to increase H_C is to produce a microstructure consisting of isolated and non-interacting FM embedded in a non-magnetic matrix. As already mentioned, this is the case of Alnico-type magnets. Moreover, in some rare-earth magnets an annealing process is used to segregate non-magnetic phases at the FM grain boundaries and thus reduce exchange interactions between them [6]. However, exchange interactions can also be beneficial in some cases, for example when hard and soft magnetic materials are coupled together, forming the so called *spring-magnets*.

1.2.2.- The concept of spring-magnet

In general, it is difficult to obtain large values of coercivity and energy product simultaneously. As seen in equation (1.1), H_C is inversely proportional to M_S . This means that hard magnetic materials, with large H_C , usually do not have as large M_S as soft magnetic materials. To overcome this difficulty, Kneller and Hawig proposed in 1991 the concept of *spring-magnet* [14]. The idea was to generate a two-phase microstructure consisting of a small proportion of soft magnetic phase embedded in a hard magnetic matrix, in such a way that both phases became strongly exchange coupled. When performing the hysteresis loop, the magnetization reverses first in the soft phase and then the domain walls propagate from the soft to the hard magnetic phase. The overall magnetic anisotropy is reduced due to the soft phase, consequently H_C usually is found to be smaller than the one of the hard phase alone. However, M_R is significantly enhanced due to the exchange interactions at the interfaces between the soft and the hard grains. These exchange interactions force the spins in each grain, specially those at the grain boundaries, to remain aligned in the direction of the previous magnetizing field, once the magnetic field is removed, thus enhancing M_R .

The first nanocomposites consisting of interacting soft and hard magnetic phases were obtained experimentally actually before the concept of spring-magnet was conceived, in 1989, by Coehoorn and co-workers who, by means of melt-spinning of $\text{Nd}_4\text{Fe}_{78}\text{B}_{18}$ synthesized a nanocomposite consisting of exchange interacting $\text{Nd}_2\text{Fe}_{14}\text{B}$, Fe_3B and $\alpha\text{-Fe}$ phases [15]. In the following years, different spring-magnets were synthesized using several techniques, such

as rapid solidification methods (e.g. melt-spinning or mechanical alloying) or chemical routes [16-19].

There are several factors which limit the magnetic properties of spring-magnets. In particular, both the mean grain size and the grain size distribution have an effect in M_R , M_R/M_S and H_C [20]. Therefore, precise control of the microstructure of the composites is required to optimise their magnetic properties.

1.3.- Phenomenology and Fundamentals of Ferromagnetic-Antiferromagnetic Coupling

1.3.1.- FM-AFM exchange anisotropy

We have already discussed two types of magnetic anisotropies in FM materials: magnetocrystalline anisotropy and shape anisotropy. Moreover, other magnetic anisotropies, such as stress anisotropy (induced by plastic deformation or mechanical tensions) or surface anisotropy may also be present in a FM material.

In 1956 a new type of magnetic anisotropy was discovered in surface oxidized Co particles [21]. This anisotropy, which is due to the interaction between AFM and FM materials (note that CoO is AFM) is usually denoted as *exchange anisotropy* or *unidirectional anisotropy* [22].

Since its discovery, this phenomenon, which has its origin in the interactions between the interfacial spins of the FM and the AFM, has been widely studied, in fine particles, bulk inhomogeneous materials, FM-AFM thin films, or thin FM films deposited on the top of AFM monocrystals [22]. The effects of exchange coupling have been also observed in ferrimagnetic-AFM and ferrimagnetic-FM materials [23,24].

1.3.2.- Phenomenology:

Ferromagnetic-antiferromagnetic exchange coupling is typically induced when a material with a certain number of FM-AFM interfaces is cooled, under the presence of a magnetic field, from a temperature T higher than the AFM Néel temperature (usually the condition $T_N < T < T_C$ has to be fulfilled) [22].

The most well-known effect of FM-AFM coupling is a shift of the hysteresis loop, along the field axis, in the opposite sense of the magnetic field applied during the cooling process. The amount of shift, usually designated by H_E , is called *exchange bias field*. Another feature of FM-AFM coupling is a widening of the hysteresis loop, i.e. an increase of H_C , especially when the AFM anisotropy is low. Both effects (loop shift and coercivity enhancement) tend to decrease with temperature, becoming zero at temperatures close to T_N , due to the loss of magnetic ordering in the AFM. Shown in figure 1.6 are typical hysteresis loops of (a) a FM material and (b) a FM material coupled to an AFM.

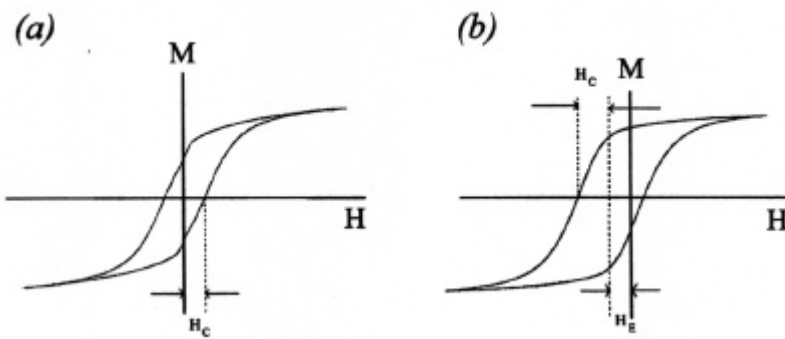


Figure 1.6: Hysteresis loops of (a) a FM material and (b) an exchange coupled FM-AFM material. It can be seen that in (b) the hysteresis loop is shifted along the field axis by an amount H_E and the coercivity, H_C , is enhanced with respect to (a).

Further evidence of FM-AFM coupling can be inferred from the curve obtained by torque magnetometry. In torque curves, the force required to rotate the magnetization of a sample out of its easy axis direction is plotted as a function of the angle of rotation [2,4]. For simplicity, let us consider the case of a disc-shaped single crystal with uniaxial anisotropy, i.e. with only one easy axis, and let us assume that the easy axis is in the plane of the disc. If the disc is then suspended in horizontal position, by means of a string, and a strong magnetic field is applied, the disc will rotate until its easy axis becomes parallel to the direction of the field. If the string is subsequently twisted, the easy axis will be at an angle \mathbf{q} out of the direction of M . It can be demonstrated that the anisotropy energy for unit volume will be given, to a first approximation, by the following expression:

$$E = K_u \sin^2 \mathbf{q} \quad (1.3)$$

where K_u is the anisotropy constant of the uniaxial crystal.

The first derivative of E with respect to \mathbf{q} gives the macroscopic torque, \mathbf{G} exerted by the external field:

$$\mathbf{G} = -\frac{dE}{d\mathbf{q}} = -2K_u \sin \mathbf{q} \cos \mathbf{q} = -K_u \sin 2\mathbf{q} \quad (1.4)$$

Shown in figure 1.7 (a) are the angular dependences of the energy and torque for a FM material with uniaxial anisotropy. As seen in the figure, there are two positions of minimum energy, for $\mathbf{q} = 0^\circ$ and $\mathbf{q} = 180^\circ$, which are positions of stable equilibrium.

Conversely, in exchange coupled FM-AFM materials, the angular dependence of \mathbf{G} is like the one shown in figure 1.7 (b). In this case, \mathbf{G} can be expressed by the following equation:

$$\mathbf{G} = -K_u \sin \mathbf{q} \quad (1.5)$$

Therefore, the unit volume anisotropy energy is given by:

$$E = K_u \cos \mathbf{q} + E_0 \quad (1.6)$$

where E_0 is an integration constant.

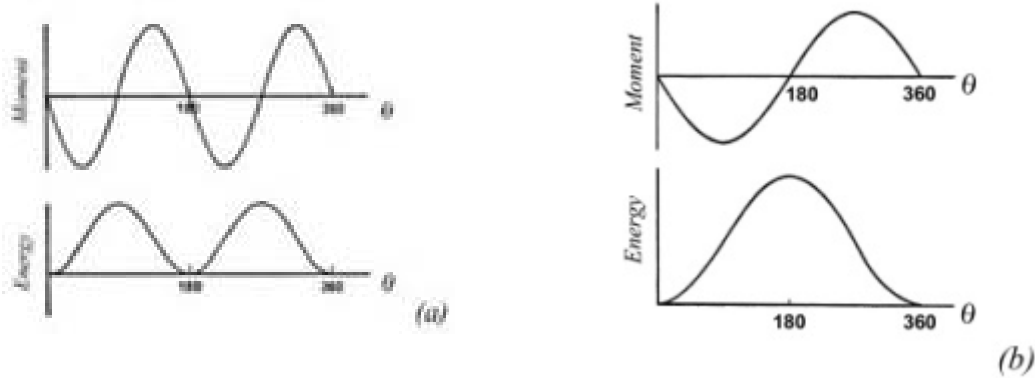


Figure 1.7: Angular dependence of the torque and energy curves in (a) a FM material and (b) an exchange coupled FM-AFM material.

Contrary to the case of an uncoupled FM material, in a FM-AFM couple, there is only one position of minimum energy. In other words, in a FM material with uniaxial anisotropy

there are two equivalent equilibrium positions at $\mathbf{q} = 0^\circ$ and $\mathbf{q} = 180^\circ$. However, in a FM-AFM couple only one of these configurations minimizes E , e.g. $\mathbf{q} = 0^\circ$ [21,22]. That is why FM-AFM exchange anisotropy is usually also designated as *unidirectional anisotropy*.

1.3.3.- Intuitive picture:

The first model to explain the existence of loop shifts and coercivity enhancements in exchange coupled FM-AFM materials was given by Meiklejohn and Bean in 1956. This model, although it is not able to quantitatively describe all the experimental results reported in the literature, it gives a good intuitive picture to understand, at least qualitatively, the physical principles of the coupling [21,25].

Shown in figure 1.8 are the spin configurations in the FM and the AFM layers, before and after a field cooling process [22]. If a magnetic field is applied at a temperature T so that $T_N < T < T_C$ and the field is large enough, all the spins in the FM will align parallel to H , i.e. the FM will be saturated. Meanwhile, the spins in the AFM will remain at random, since $T > T_N$. When the FM-AFM couple is cooled through T_N , the magnetic order in the AFM is set up. During the cooling, it is likely that, at the FM-AFM interface, the spins of both components interact with each other. If so, the first layer of spins in the AFM will tend to align parallel to the spins in the FM (assuming ferromagnetic interaction at the interface), while the successive remaining layers in the AFM will orient antiparallel to each other, so as to give a zero net magnetization in the AFM.

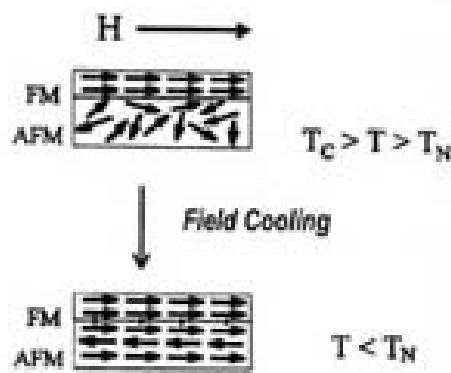


Figure 1.8: Schematic diagram of the spin configurations in a FM-AFM bilayer, before and after a field cooling process [22].

Within this model, two different opposite cases can be predicted, depending on the AFM magnetic anisotropy. If the AFM anisotropy is low, one should only observe a coercivity enhancement (without any loop shift), while for large AFM anisotropies, the only observed effect should be a shift of the hysteresis loop. Nevertheless, in general, both effects can be observed simultaneously, because, for example, structural defects or grain size distribution bring about local variations of the AFM anisotropy.

The spin configuration, for a FM-AFM couple, is shown schematically in figure 1.9 for different stages of a hysteresis loop [22]. After the field cooling process, the spins in both the FM and the AFM lie parallel to each other (a). When the magnetic field is reversed, the spins in the FM start to rotate. However, if the AFM anisotropy is large enough, the spins in the AFM will remain fixed. Consequently, due to the coupling, they will exert a microscopic torque to the spins in the FM, trying to keep them in their original position (b). Thus, the magnetic field required to completely reverse the magnetization in the FM will be higher than if the FM was not coupled to an AFM, i.e. an extra magnetic field will be required to overcome the microscopic torque due to the spins in the AFM. And, as a result, the coercivity in the negative field branch increases (c).

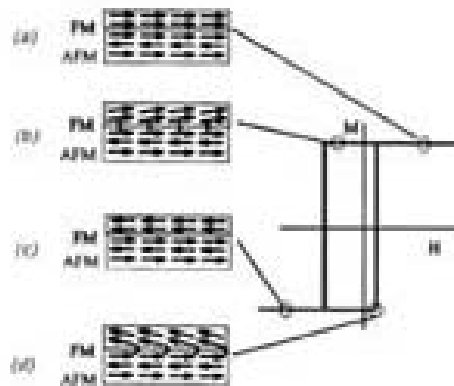


Figure 1.9: Schematic diagram of the spin configurations of a FM-AFM couple at the different stages of a shifted hysteresis loop [22].

Conversely, when the magnetic field is reversed back to positive values, the rotation of spins in the FM will be easier than in an uncoupled FM, since the interaction with the spins in the AFM will favour the magnetization reversion, i.e. the AFM will exert a microscopic torque in the same direction as the applied magnetic field (d). Therefore, the coercivity in the positive fields branch will be reduced. The net effect will be a shift of the hysteresis loop along the magnetic field axis. Thus, the spins in the FM have only one stable configuration (unidirectional anisotropy).

When the AFM anisotropy is low the situation is different (see figure 1.10). As in the previous case, after the field cooling, the spins in both layers are aligned in the same direction (a). However, when the magnetic field is reversed and the spins in the FM start to rotate, if the AFM anisotropy is too low, the spins in the AFM can be dragged by the spins in the FM (b). In other words, it will be energetically more favourable that the spins in both the FM and the AFM rotate together. However, the AFM spins rotate to a certain angle and finally reach a stable configuration, inducing the necessary irreversibility to induce increased coercivity. An analogous behaviour will be observed after saturating in negative fields ((c) and (d)).

In this case, although no loop shift will be observed, the magnetic field required to reverse magnetizations in both positive and negative branches will become larger, i.e. an extra energy will be required. Consequently, the hysteresis loop will widen and the coercivity will be enhanced.

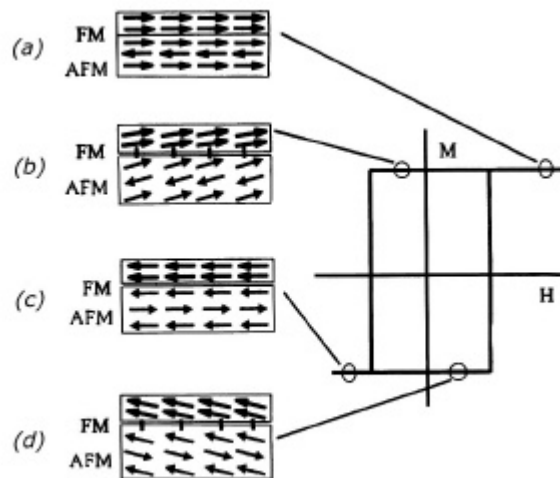


Figure 1.10: Schematic diagram of the spin configurations of a FM-AFM bilayer, at the different stages of a widened hysteresis loop due to the exchange interactions.

Although this phenomenological model gives quite an intuitive and simple image of FM-AFM coupling, it is true that it has serious deficiencies, since it does not consider some key points, such as for example the role of the FM anisotropy in the coupling, the effects of interface roughness, the presence of structural defects or the formation and motion of domain walls.

1.3.4.- Theoretical outline:

The model described in the preceding section was the first theoretical approach to exchange bias phenomena. Two of the main assumptions of the model are that the magnetization rotates coherently and the FM and AFM easy axis are parallel. The energy per surface unit in the FM-AFM couple can be expressed by [25]:

$$E = -HM_{FM}t_{FM} \cos(\mathbf{q} - \mathbf{b}) + K_{FM}t_{FM} \sin^2(\mathbf{b}) + K_{AFM}t_{AFM} \sin^2(\mathbf{a}) - J_{INT} \cos(\mathbf{b} - \mathbf{a})$$

(1.7)

where H is the applied magnetic field, M_{FM} is the saturation magnetization in the FM, t_{FM} and t_{AFM} are the thicknesses of the FM and AFM layers, K_{FM} and K_{AFM} are the magnetic anisotropies in the FM and the AFM and J_{INT} is the exchange coupling constant at the interface. The angles \mathbf{a} , \mathbf{b} and \mathbf{q} are, respectively, the angles between the planes of spins in the AFM and the AFM easy axis, the direction of the spins in the FM and the FM easy axes and the direction of H and the FM easy axis (see figure 1.11).

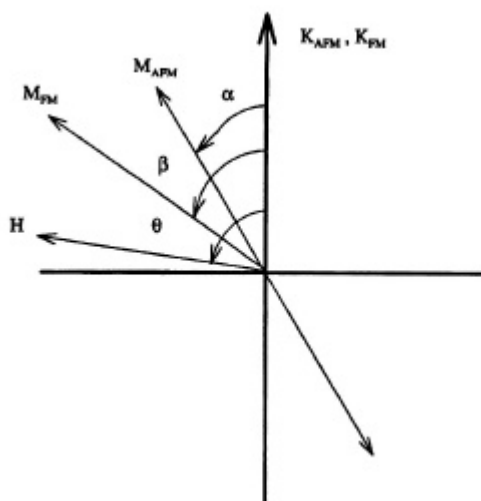


Figure 1.11: Schematic diagram of the angles involved in a FM-AFM exchange coupled system. It is assumed that the easy axis in the FM and AFM layers are collinear.

It can be seen from equation 1.7 that if no coupling exists between the FM and the AFM and the applied magnetic field becomes zero, the overall energy of the FM-AFM system reduces to the terms due to the AFM and the FM magnetic anisotropies (2nd and 3rd terms). However, if a magnetic field is applied, a certain work has to be carried out to rotate the spins in the FM (1st term). Finally, the 4th term represents the FM-AFM coupling. From equation 1.7 one can easily deduce, in first approximation, the value of the exchange bias, H_E , if some assumptions are made. For example, let's first assume that the field is applied along the FM easy axis, i.e. $\mathbf{q} \rightarrow 0$. Secondly, let's suppose that the AFM anisotropy constant is very large, so that the spins of the AFM do not rotate with the field (i.e. they keep aligned along the AFM easy axis, so that $\mathbf{a} \sim 0$ and $\sin^2(\mathbf{a}) \sim 0$). Then eq. 1.7 can be rewritten as follows:

$$E = -HM_{FM}t_{FM} \cos(\mathbf{b}) - J_{INT} \cos(\mathbf{b}) + K_{FM}t_{FM} \sin^2(\mathbf{b}) \quad (1.8a)$$

which leads to:

$$E = -(HM_{FM}t_{FM} + J_{INT}) \cos(\mathbf{b}) + K_{FM}t_{FM} \sin^2(\mathbf{b}) \quad (1.8b)$$

This equation is analogous to the Stoner-Wohlfarth equation of energy for single-domain, non-interacting particles, with uniaxial anisotropy, i.e. [3]:

$$E = -(H_{eff}M_{FM}t_{FM}) \cos(\mathbf{b}) + K_{FM}t_{FM} \sin^2(\mathbf{b}) \quad (1.9)$$

From equation 1.9 By plotting E as a function of \mathbf{b} and looking for stability for different values of H , it is possible to determine numerically the value of H_C , which has been given in equation 1.1, i.e. $H_C = \frac{2K_{FM}t_{FM}}{M_{FM}t_{FM}}$.

Note that equations 1.8(b) and 1.9 are identical if $H_{eff} = H + \frac{J_{INT}}{M_{FM}t_{FM}}$. This indicates that, under these assumptions, the hysteresis loop of the FM-AFM system will be shifted by the amount $H_E = \frac{J_{INT}}{M_{FM}t_{FM}}$ along the magnetic field axis.

Note that, although this formula takes into account some relevant physical parameters of the FM-AFM couple, it assumes, among other factors, a lack of domain structure in the FM

and the AFM, co-linearity of the FM and AFM easy axes and absence of structural defects at the interface. Furthermore, it neglects the effect that the magnetic field may have on the spins in the AFM and the possibility of having a completely compensated spin structure in the first layer of spins in the AFM at the interface. Note that a compensated spin structure in the first layer of the AFM means that the spins in this layer are aligned alternatively in opposite directions, so that the net magnetization in the first layer of the AFM is zero.

It is noteworthy that if the magnetic anisotropy in the AFM is low (usually this is expressed by $K_{AFM} t_{AFM} < J_{INT}$) it is energetically more favourable that during the hysteresis loop the spins in the FM and the AFM rotate together, i.e. $(\mathbf{b} - \mathbf{a}) \sim 0$. Then, assuming that H is applied along the FM easy axis, equation 1.7 can be rewritten as follows:

$$E = -HM_{FM} t_{FM} \cos(\mathbf{b}) + K_{FM} t_{FM} \sin^2(\mathbf{b}) + K_{AFM} t_{AFM} \sin^2(\mathbf{b}) - J_{INT} \quad (1.10)$$

Therefore:

$$E = -HM_{FM} t_{FM} \cos(\mathbf{b}) + (K_{FM} t_{FM} + K_{AFM} t_{AFM}) \sin^2(\mathbf{b}) - J_{INT} \quad (1.11)$$

In this case, comparing with equation 1.9, one can observe that $H = H_{eff}$, i.e. there is no loop shift. However, the value of H_C will change, since the overall magnetic anisotropy is modified due to the coupling (see equation 1.1).

Nevertheless, it has to be mentioned that in the framework of Meiklejohn's model it is not possible to predict the observed enhancement of coercivity in exchange interacting FM-AFM couples. Moreover, within this model, choosing appropriate values of the interface exchange constant, J_{INT} , the values predicted for H_E are usually several orders of magnitude larger than the experimental results [26]. Therefore, several authors have developed more complex models, in which many other effects are taken into account. Hence, for example, some models include the effects of the external magnetic field on the AFM [27], the effect of grain size distribution on the FM-AFM coupling [28], the non-collinearity of spins in the FM and AFM layers [29], the spins compensation in the first layer of the AFM [30] or the random anisotropy generated in the AFM, due to the presence of surface roughness at the interface [31] or diluted antiferromagnets [32].

Some models emphasize the importance that the existence of magnetic domains in the AFM can have on the coupling. In this sense, A.P. Malozemoff assumed that, when performing a hysteresis loop of a FM-AFM couple, some domain walls were created in the

AFM, perpendicularly to the interface, due to the random fields generated as a consequence of surface roughness or other defects at the interface [31]. According to Malozemoff, the uncompensation of spins due to the AFM magnetic domain structure is mainly responsible for the existence of H_E . Conversely, D. Mauri and N.C. Koon noticed that the formation of domain walls in the AFM, parallel to the interface, could also result in a bias of the hysteresis loop [33]. Furthermore, in Koon's model it was shown that in a completely compensated AFM spin configuration at the interface, the energy is minimized when they are oriented not parallel but perpendicular to the spins in the FM [33]. This is sometimes called *perpendicular coupling*. Nevertheless, T.C. Schulthess and W.H. Butler have recently demonstrated that Koon's model does not actually predict the existence of H_E but only some enhancement of H_C , due to an increase of the uniaxial anisotropy [34]. Moreover, K. Takano et. al have recently proposed that H_E originates mainly as a consequence of non-compensated interfacial spins in the AFM [30]. They have shown that the temperature dependence of the remanent moment due to the uncompensated spins is similar to the one of H_E , concluding that both effects are closely related to each other.

There are a few models, like the one purposed by M. Kiwi et al., which consider that the effects of the coupling can be due to incomplete domain structure formation in the FM during the field cooling process, basically due to the development of metastable spin configurations at the interface of the FM [35].

Furthermore, M.D. Stiles and R.D. McMichael have reported a model to account for the effects of FM-AFM coupling in polycrystalline FM-AFM bilayers, in which the FM interacts with independent AFM grains (non-interacting) [36]. However, this model has the drawback that it assumes that the crystallites in the AFM are so small that no domain structure can be formed in the AFM.

Moreover, R.E. Camley et al. have performed some numerical simulations, in which, instead of minimizing the overall energy of the FM-AFM couple, they study the temporal evolution of the magnetization during the hysteresis loop [37]. This model predicts a spin structure in the AFM and FM layers similar to that of Koon's model and it shows that the main effect for large K_{AFM} is the existence of H_E , while for low K_{AFM} only an enhancement of H_C should be observed. In addition, this model emphasizes the importance of the applied field direction, with respect to the FM easy axis, in exchange bias and predicts different mechanisms for magnetization reversal, depending on the intensity of the magnetic field. It is noteworthy that different mechanisms of magnetization reversal have been observed also experimentally by several authors [38].

In conclusion, although all these models have succeeded, to some extent, explaining a large variety of experimental results and observations, a complete theory, able to predict all exchange bias related phenomena, is still lacking. This is because usually the models are only applicable to some particular type of materials or cases and can not be generalized to other systems.

1.4.- Ferromagnetic-Antiferromagnetic Coupling in Nanostructures and Fine-Particle Materials

Since the discovery of exchange anisotropy in 1956 in surface-oxidized cobalt fine powders [21], the effects of FM-AFM coupling have been observed in a large variety of different materials, mainly consisting of small particles, thin films, coated AFM single crystals or materials without a well defined FM-AFM interface (inhomogeneous materials) [22]. However, since the discovery of spin valves based on exchange bias and its significant applications in magnetic storage devices, the bulk of exchange bias research has concentrated in thin film systems [22,39]. Moreover, the amount of research in fine particle systems has become scarce, due to the intrinsic difficulty in controlling several physical parameters which directly affect the magnitudes of loop shifts and coercivity enhancements.

1.4.1.- Exchange bias in “artificially-fabricated” magnetic nanostructures

Recently, some work is also being carried out in artificially-fabricated FM-AFM nanostructures. By “artificially-fabricated”, we mean nanostructures grown controllably by different lithography methods. Several types of FM-AFM nanostructures are worth studying or are actually being studied at present (see figure 1.12): oxidized arrays of nanoparticles (a) [40,41], FM-AFM nanoparticles (b) [42-44] or FM nanoparticles on continuous AFM layers (c). Coercivity enhancements and loop shifts have been observed in these systems, which make them promising candidates to solve some of the miniaturization trends of the recording industry [40-44]. Although type (a) is similar to random particles, types (b) and (c) solve many of the problems of exchange bias in fine particles, since in these systems many structural parameters can be precisely controlled. Thus, these FM-AFM nanocomposites are ideal systems for theoretical modelling of the exchange bias phenomena since, by controlling the size of the particles (or dots) it is possible, in some cases, to tune the magnetic domain structure in both the FM and the AFM and, thus, corroborate or invalidate some of theoretical predictions on the exchange bias phenomena [40-45]. However, in these patterned elements, some effects due to shape anisotropy or dipolar interactions, are also usually present. This requires accurate control of some parameters, such as the separation between dots or the element aspect ratio, in order to isolate the effects of exchange bias from other effects.

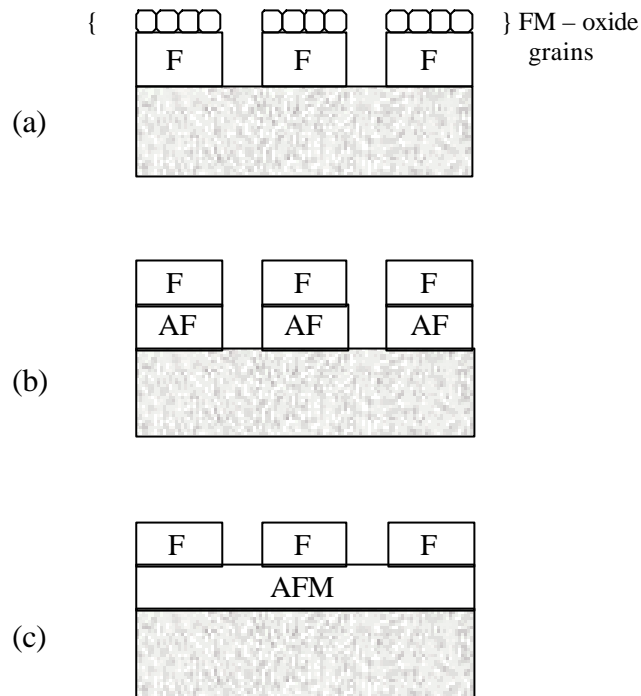


Figure 1.12: Schematic configurations of three different artificially fabricated FM-AFM nanostructures: oxidized arrays of nanoparticles (a), FM-AFM nanoparticles (b) and FM nanoparticles on continuous AFM layers (c).

1.4.2.- Exchange bias in fine powders systems

Since their discovery, exchange bias phenomena have been studied in a large number of FM-AFM fine particle systems: Co-CoO [45], Ni-NiO [46], Fe-FeO [47], Fe-Fe₃O₄ [48], Fe-FeS [49], Fe-Fe₂N [50], Co-CoN [51], etc. These particles are usually in the nanometer range (5-100 nm) and typically exhibit a core-shell microstructure, in which a FM inner core is surrounded by an oxide, nitride or sulphide surface layer, obtained either by natural oxidation or chemical treatments of the particles. Several techniques allow the processing of this kind of materials. Among them, vapour deposition, chemical reduction, gas condensation, aerosol spray pyrolysis or mechanical alloying are the most frequently used [22,52].

Although loop shifts have been observed in FM-AFM fine particles, the main characteristic of these systems is the enhancement of the coercivity occurring at $T < T_N$. Consequently, exchange bias was suggested as a possible route for permanent magnet processing. However, in fine-particle systems, the properties of exchange bias are only usually observed for temperatures below room temperature. This is in part because many

AFM have Néel temperatures below room temperature (e.g. FeO, CoO). In addition, the reduced size of the AFM crystallites also limits the temperature range in which the interactions can occur. When the AFM grain size becomes increasingly small, thermal fluctuations cause a loss of the AFM magnetic ordering, i.e. they become superparamagnetic. When heating a FM-AFM couple, the temperature at which the effects of the coupling disappear is called *blocking temperature* and is designated as T_B . It has been found experimentally that T_B is progressively reduced as the AFM grain size or thickness decreases [53,54]. However, the main reason of the limited research in exchange biased particles is that these systems are not ideal for studies of fundamental aspects of exchange bias, since distributions of particle sizes and shapes are always present. Moreover, it is very difficult to control some key parameters which play an important role in the FM-AFM coupling, such as AFM or FM layer thicknesses, interface roughness, crystallinity, stoichiometry, etc. Finally, from a technological point of view, the fact that the AFM phases are usually formed or derived from the FM cores represents a severe limitation to the number of systems in which FM-AFM interactions can be induced. For instance, in general, it is difficult to obtain AFM phases by chemically treating the surface of hard magnetic particles.

Moreover, some interest has arisen in *pure* FM, AFM and ferrimagnetic nanoparticles, since sometimes they also exhibit loop shifts and coercivity enhancements [55,56]. These effects are generally attributed to the existence of a spin-glass-like layer surrounding each particle due to surface disorder (e.g. uncoupled spins or roughness). During a field cooling process, the spin-glass layer can become “frozen” and thus couple to the AFM, FM or ferrimagnetic cores. Note that, due to the random magnetic configuration, spin glasses can play the role of both FM and AFM in FM-AFM coupling [22].

1.5.- Objectives of our Work

As already mentioned, traditionally, most of the studies on FM-AFM coupling in fine particles have been carried out in FM and AFM usually derived from the same transition metal (e.g. between Fe and Fe-based AFM) [22]. This is a severe limitation for the technological applications of the exchange bias phenomena, mainly due to the difficulty of deriving AFM phases from hard magnetic materials.

Moreover, although, as observed in thin films, many fine particles exhibit loop shifts, the most noticeable aspect of exchange bias in fine particles is the coercivity enhancement [22]. However, this enhancement is usually only observed at low temperatures, either because the AFM shells have T_N below room temperature or because their crystallites are so small that they behave superparamagnetically at room temperature. Thus, considering previous results,

to make use of the coercivity enhancement to improve the quality of the permanent magnetic materials commonly used in the industry could have been deemed as virtually impossible.

To overcome all these difficulties, in the present work, we utilize ball milling as a processing technique to induce FM-AFM exchange interactions at room temperature. This is achieved by mixing FM with AFM materials, whose Néel temperature is above room temperature. Moreover, FM-AFM coupling can be induced in combinations of AFM and FM powders not derived from the same transition metal (e.g. in Co with NiO or in Co with FeS) or even between hard FM and AFM particles (e.g. in SmCo_5 with NiO). Ball milling of the two components is shown to result in an enhancement of the coercivity and the squareness ratio with respect to the FM phase alone. Besides, by optimizing the FM:AFM percentages and the milling conditions it is possible to achieve an improvement of the energy product, which is more closely related to the quality of a permanent magnet. Finally, this procedure has been chosen due to its simplicity and relatively low price, which makes it easily scaleable to industrial production.

Note that due to the different magnitude of the magnetic fields involved in the two systems studied (e.g. Co + NiO and SmCo_5 + NiO), although in the thesis the magnetic units have been kept in cgs units (e.g. H_C in Oe, $(BH)_{Max}$ in G Oe) in the articles concerning SmCo_5 + NiO the coercivity and energy product are given in the SI unit system (e.g. mH_C in T, $(BH)_{Max}$ in kJ/m^3).